SURFACE AND INTERFACE ANALYSIS
Surf. Interface Anal. 2006; **38**: 1242–1246
Published online 19 June 2006 in Wiley InterScience
(www.interscience.wiley.com) DOI: 10.1002/sia.2386

Surface and Interface Analysis

Ultrasound-assisted oxidation of tungsten in oxygen plasma: the early stages of the oxide film growth

Andriy Romanyuk,[1]* Roland Steiner,[1] Viktor Melnik[2] and Verena Thommen[1]

[1] University of Basel, Institute of Physics, Klingelbergstrasse 82, 4056 Basel, Switzerland
[2] IHP - Microelectronics, Im Technologiepark 25, 15236 Frankfurt (Oder), Germany

Received 9 March 2006; Revised 24 April 2006; Accepted 24 April 2006

The effect of ultrasonic vibrations applied *in situ* on the formation of W–WO interface during the exposure of a pure tungsten foil to a low-temperature oxygen plasma is investigated by photoelectron spectroscopy (XPS) and time-of-flight secondary ion mass spectrometry (TOF-SIMS). The tungsten surface was exposed to oxygen plasma at different time intervals and the evolution of the interface formation was studied by angle-resolved XPS. We show that oxidation without ultrasonic vibrations leads to the formation of a thin oxide film whose growth kinetics is governed by an island growth mechanism. On the other hand, oxide growth in the presence of ultrasonic treatment (UST) appears to follow a layer-by-layer growth mode with a distinctly sharper W–WO interface. TOF-SIMS analysis in this case revealed a reduced amount of water bonded in the film, which suggests an increase in the film's packing density. Copyright © 2006 John Wiley & Sons, Ltd.

KEYWORDS: oxidation; tungsten oxide; growth mechanism; secondary ion mass spectrometry (SIMS); X-ray photoelectron spectroscopy (XPS)

INTRODUCTION

Transition-metal oxides have attracted considerable attention for their potential applications as catalysts and active materials in smart windows technology.[1–4] The investigation of the properties of oxides is of great importance in the application of these materials and has been the subject of many research studies (Refs 5–7 and references therein). However, the dramatic charging problem may severely hamper the study of oxides by surface science techniques based on electron/photon emission processes. In this case, oxide thin films on metallic substrates can be used as model systems to study the surface properties of highly insulating oxides.[7–9] The preparation of ultrathin metal oxide films for surface science studies has been carried out most frequently by oxidizing a metal substrate, thereby forming a thin film of the native oxide. However, with this method difficulties may arise in the control of film thickness and stoichiometry. Over the last few years, novel methods for metal oxidation such as ion beam and plasma oxidation have attracted considerable attention.[10–12] The oxidation of tungsten in low-temperature oxygen plasma has been studied by several authors.[13–15] In our previous work, we have shown that lattice excitations by ultrasonic vibrations applied *in situ* result in a significant decrease of the oxide thickness and in a distinctly sharper W–WO interface.[15] The effect was attributed to different nucleation and growth kinetics of the oxide film.

*Correspondence to: Andriy Romanyuk, University of Basel, Institute of Physics, Klingelbergstrasse 82, 4056 Basel, Switzerland.
E-mail: andriy.romanyuk@unibas.ch

In order to gain a deeper understanding of oxide growth kinetics, two complementary analytical techniques have been used in the present work: time-of-flight ion mass spectrometry (TOF-SIMS), and angle-resolved X-ray photoelectron spectroscopy (ARXPS), which allows in-depth distribution analysis of chemical composition in outermost layers of the solid to be performed.

EXPERIMENTAL DETAILS

Substrates of polycrystalline tungsten foil ($10\times10\times0.05$ mm^3 from Goodfellow, 99.99% pure) were polished using a standard electrochemical mechanical polishing procedure as described elsewhere.[16] The surface roughness after polishing, measured with AFM and defined as an arithmetic average of the absolute values of the surface height deviations, was found to be ~2 nm. Prior to oxidation, the sample was successively subjected to Ar^+ sputtering and heating in vacuum in order to remove surface contaminations. The samples were then oxidized in a low-temperature reactive oxygen r.f. plasma at different time intervals at 50 W and a pressure of 0.5 Pa. The electrode, to which the power is applied, consists of a graphite-covered tantalum sheet, whereas the grounded electrode holds the water-cooled substrate. The gas composition in the experimental chamber during plasma discharge, measured with a differentially pumped quadrupole mass spectrometer (Prisma QMS100, Pfeiffer Vacuum), mainly consisted of O and O_2 as well as some amount of hydrogen and CO. The ultrasonic vibrations were generated in the sample *in situ*, i.e. during the oxidation process, by operating the transducer in a resonant vibration

Copyright © 2006 John Wiley & Sons, Ltd.

WILEY InterScience® DISCOVER SOMETHING GREAT

mode at a resonance frequency of 5 MHz and an acoustic power of 1 W cm^{-2}.

The samples were then transferred into the XPS analyzing chamber without breaking the vacuum under a background pressure below 1×10^{-7} Pa. ARXPS core-level spectra were measured with a VG ESCALAB 210 spectrometer equipped with a monochromatized Al Kα (1486.6 eV) radiation source, between normal (0°) and grazing (80°) emission angles. The energy position of the spectra were calibrated with reference to the Au $4f_{7/2}$ level of a clean gold sample positioned at 84.0 eV binding energy. In order to obtain the peak intensities, a numerical least-squares fitting procedure[17] using Doniach–Sunjic line shapes[18] was applied after a Shirley background substraction.[19]

TOF-SIMS measurements were performed on an IONTOF IV instrument in a dual-beam mode with a 10 keV Ar^+ primary beam and a 0.6 keV Cs^+ sputtering beam.

RESULTS AND DISCUSSION

XPS analysis

The evolution of the W 4f core-level spectra (normal emission) for different oxygen plasma exposure times is depicted in Fig. 1(a) (normal oxidation, i.e. without ultrasonic treatment (UST)) and Fig. 1(b) (oxidation with UST). The W 4f line measured on the pure polycrystalline foil consists of one doublet at binding energy 31.15 eV for the W $4f_{7/2}$ doublet component and spin–orbit splitting Δ_E of 2.15 eV. Exposure of the metal surface to the oxygen plasma results in surface oxidation, which can be seen in the appearance of a second doublet with W $4f_{7/2}$ line at 35.28 eV and spin–orbit splitting energy of 2.14 eV. This doublet is associated with the oxidation state W^{6+}, and its intensity increases with the plasma exposure time in both oxidation techniques. It is worth mentioning that no lower oxidation states are observed, which could be explained by a high amount of reactive oxygen species in the plasma and an essential difference in enthalpy of oxide formation at room temperature.[20]

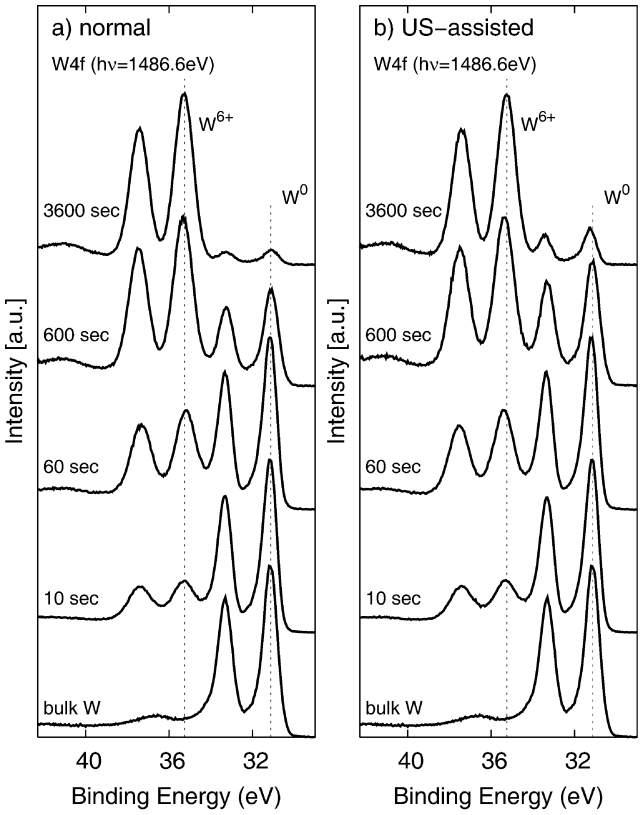

Figure 1. Evolution of the W 4f spectra taken at normal emission for different oxidation times: (a) without ultrasonic vibrations, (b) with ultrasonic vibrations applied *in situ*. The bottom most spectra correspond to the measurement of the initial tungsten foil.

In order to investigate the early stages of film growth, ARXPS measurements were used. Figure 2 shows the initial stages of film formation and the ARXPS experiment geometry. This technique allows the layer sequence at the very beginning of film growth to be analyzed by varying the surface sensitivity (i.e. the information depth) by tuning the detection angle of the emitted photoelectrons. Line shape analysis for the measured W $4f_{7/2}$ line in W^0 and W^{6+} states was performed; this allowed reliable values for the peak intensities to be obtained. The results of this procedure are summarized in Fig. 3, where the ratio of integrated intensities of the metal substrate (W^0) and oxide overlayer (W^{6+}) is plotted for various emission angles for normal (filled symbols) and US-assisted (open symbols) oxidation and for plasma exposure times of 10 s (a) and 60 s (b). The angular dependencies of the W $4f_{7/2}$ integrated areas depicted in Fig. 3 have similar behavior in both oxidation methods, showing a decreasing contribution of the metal component with increasing detection angle φ due to the enhanced attenuation of photoelectrons emitted from the underlying metal substrate. In order to gain information about the oxide's growth mechanism, the experimental intensity ratios were compared with theoretically calculated ratios using standard formulas for angle-resolved photoemission.[21,22] The curves were fitted with a least-squares procedure using film thickness and coverage as fit parameters while keeping the value of the electron inelastic mean free path (IMFP) constant at 2.8 nm (the value of IMFP was derived from the predictive equation of Gries[23]). The best fit to the measured data shown in Fig. 3 (symbols) and calculations (lines) is obtained with the parameter set presented in Table 1. As can be seen in the

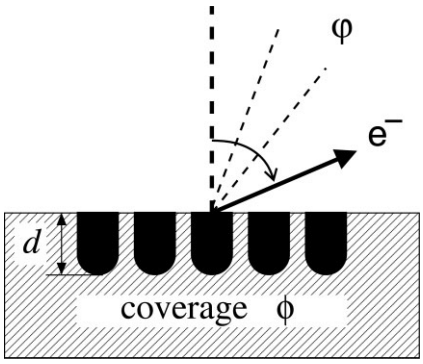

Figure 2. Schematic view of a thin film formation stage and geometry of an ARXPS experiment; the emission direction of the photoelectron is specified by the polar angle φ.

Copyright © 2006 John Wiley & Sons, Ltd.

DOI: 10.1002/sia

Surface and Interface Analysis

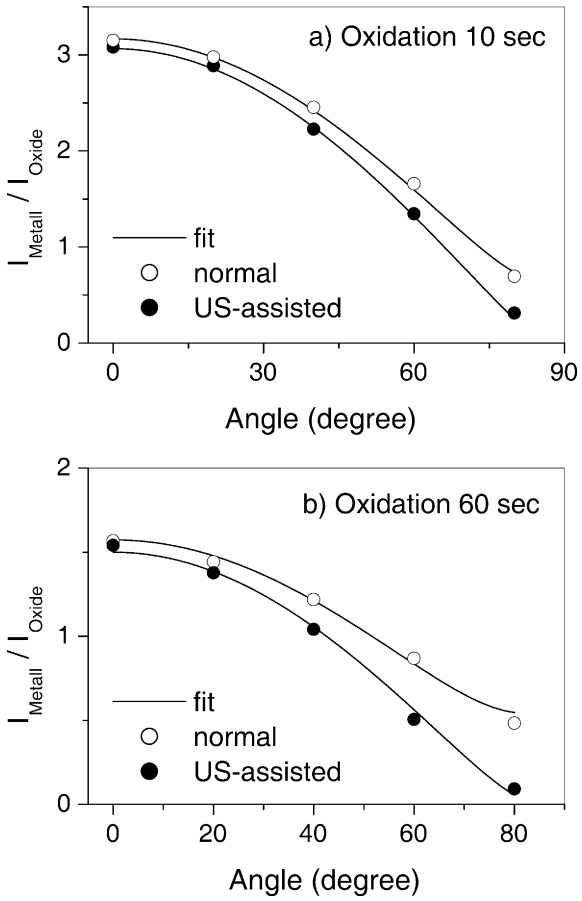

Figure 3. Ratio of the metal and oxide W $4f_{7/2}$ integrated areas as a function of the photoelectron detection angle for the oxidation time (a) 10 s and (b) 60 s. Experimental data as determined by a line shape analysis of the measured core-level spectra for normal oxidation (open symbols) and US-assisted oxidation (filled symbols); theoretical values as calculated from the parameter set presented in Table 1 (solid lines).

case of normal oxidation, the coverage and film thickness values (Table 1) lend support to the Volmer–Weber growth mode, in which the deposits form multilayer conglomerates (island growth). In clear contrast, the results obtained for US-assisted oxidation are close to those predicted for Frank–van der Merve (layer-by-layer) growth with a coverage of nearly 100% for both oxidation times. Oxidation for 3600 s results in the formation of closed films for both oxidation methods as exemplified by TEM measurements reported in our previous work[15] with an oxide thickness of ~11 nm for normal oxidation and ~5 nm for US-assisted oxidation.

TOF-SIMS measurements

Figure 4(a) shows the distribution of $[WO_3]^{232}$ fragment ions measured with TOF-SIMS on an oxidized tungsten surface without acoustic vibrations (open symbols) and with UST applied *in situ* (filled symbols) for a plasma exposure time of 3600 s. The position of the W–WO interface is determined (i) by the point where the $[WO_3]^{232}$ signal is at 50% of its maximum intensity and (ii) from the maximum yield of $[WO_2]^{216}$ and $[WO]^{200}$ complexes (not shown here). The latter characterizes the change of environment of the tungsten atom which takes place at the interface. The thickness

Table 1. Simulation parameters used in the formulas for angle-resolved photoemission

		Oxidation 10 s	Oxidation 60 s	Oxidation 3600 s
With UST	Oxide coverage (%)	99	100	100
	Oxide thickness (nm)	0.8	1.4	5
Without UST	Oxide coverage (%)	61	65	100
	Oxide thickness (nm)	1.4	2.5	11

of the film estimated with these methods is found to be about 12 nm for normal oxidation, whereas in ultrasonically-assisted oxidation the film thickness is only ~5 nm, which is in excellent agreement with the information deduced from the XPS measurements.

In Fig. 4(b), the $[OH]^{17}$ profiles measured for normal (open symbols) and ultrasonically-assisted (filled symbols) oxidation methods are compared. A significantly reduced yield of $[OH]^{17}$ fragment ions is evident in case of ultrasonically-assisted oxidation. It is most likely that the OH groups get incorporated into the oxide film after the exposure of the sample to the atmosphere, as the amount of OH in the gas composition according to the mass spectrometry analysis is negligible. Therefore, the decrease in OH content in the tungsten oxide films can be interpreted by an increase in the packing density of the films, i.e. the films oxidized without the acoustic vibrations are porous, whereas the films oxidized with applied ultrasound treatment possess denser, less porous structures. This conclusion is in good agreement with the data published previously about the influence of water partial pressure on the density of evaporated WO_3 films.[24]

Figure 5(a) shows the AFM image taken of the sample oxidized without UST for a plasma exposure time of 3600 s. Normal oxidation does not change the surface morphology as compared to the pristine, i.e. unexposed, sample (not shown here) and is characterized by a similar value of the surface roughness (~2.1 nm). In clear contrast to the normal oxidation, the presence of acoustic vibrations leads to the formation of an oxide film with substantially changed surface structure (Fig. 5(b)). The respective surface roughness value is found to be ~0.8 nm.

It can therefore be inferred that the formation process of thin oxide films under the action of acoustic vibrations is different from their growth under normal conditions. In the latter case, the oxide phase nucleates and grows locally on the surface with an island character. With increase of oxidation time the individual islands continue to grow until they become so large that they touch one another. At this stage an interlinking network of islands is formed, separated by 'valleys' of the substrate. The valleys are then slowly filled in until a single continuous film is formed. Ultrasonically-assisted oxidation is likely to have a different growth kinetics. UST leads to the breaking of the

Copyright © 2006 John Wiley & Sons, Ltd.

DOI: 10.1002/sia

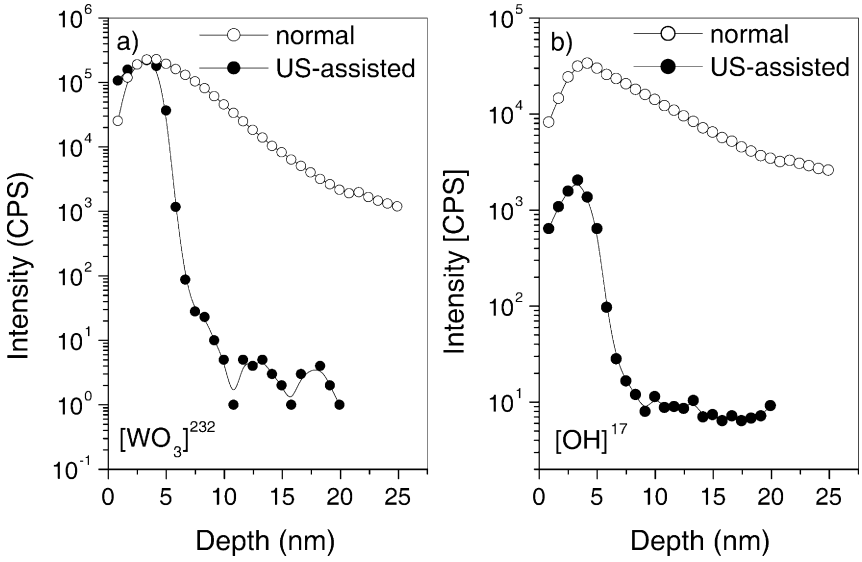

Figure 4. TOF-SIMS depth profiles of (a) $[WO_3]^{232}$ and (b) $[OH]^{17}$ in a tungsten foil exposed to oxygen plasma without UST (open symbols) and with UST applied *in situ* (filled symbols) for 3600 s.

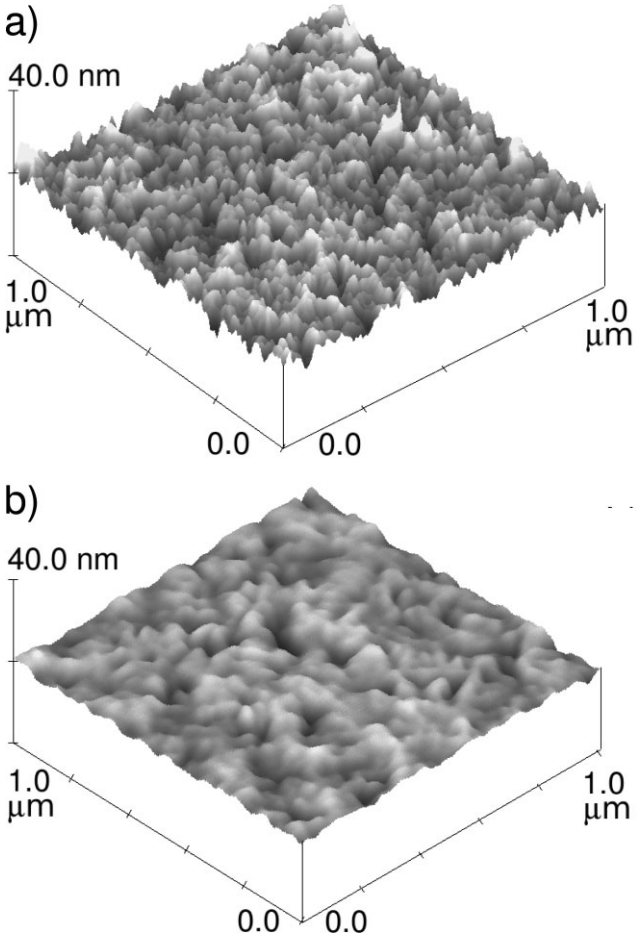

Figure 5. AFM images of the tungsten surface exposed to oxygen plasma without UST (a) and with UST applied *in situ* (b) for 3600 s.

weakest W–O bonds resulting in a stunted island creation which consequently leads to continuous film growth at the whole surface. Owing to such a mechanism, the film grows uniformly with higher density, which is reinforced by the significantly reduced structural water in the film observed by SIMS. Oxygen diffusion through such a film is substantially reduced resulting in a decrease in the film thickness.

The microscopic mechanism responsible for the different growth kinetics has been discussed previously.[15] It includes ultrasonically stimulated defects diffusion and decrease in mechanical stress in subsurface metal layers. It is also possible for ultrasonic vibrations to be transmitted into the plasma, resulting in a change of various plasma properties such as electron and ion temperature, plasma density, etc. On the basis of present knowledge, the microscopic picture still remains unclear and will be investigated further.

CONCLUSIONS

We have presented a comparative study of the interface formation between tungsten and tungsten oxide in reactive oxygen plasma with ultrasonic vibrations applied *in situ*. Oxidation of the tungsten surface in the absence of ultrasonic vibrations results in film formation whose growth mechanism appears to have an island character. Under these growth conditions, enhanced oxygen diffusion exists at the grain boundaries, which results in the formation of a smooth W–WO interface. On the contrary, acoustic vibrations lead to homogeneous film nucleation, thus decreasing oxygen diffusion through the film. The latter results in growth of a continuous film with significantly reduced water content and a sharper oxide–metal interface. Future experiments will allow us to extend this experiment to gain an improved understanding of the influence of different parameters, such as ultrasonic frequency or acoustic power.

Acknowledgements

The authors wish to thank Dr Teresa de los Arcos for a careful reading of the manuscript. Financial support of the Swiss Federal Office of Energy is gratefully acknowledged.

Copyright © 2006 John Wiley & Sons, Ltd.

DOI: 10.1002/sia

Surface and Interface Analysis

REFERENCES

1. Granqvist CG. *Handbook on Inorganic Electrochromic Materials*. Elsevier: Amsterdam, 1995.
2. Greenberg CB. *Thin Solid Films* 1994; **251**: 81.
3. Lampert CM. *Sol. Energy Mater. Sol. Cells* 1998; **52**: 207.
4. Bange K. *Sol. Energy Mater. Sol. Cells* 1999; **58**: 1.
5. Kung HH. *Transition Metal Oxides: Surface Chemistry and Catalysis*. Elsevier: Amsterdam, 1988.
6. Henrich VE, Cox PA. *The Surface Science of Metal Oxides*. Cambridge University Press: Cambridge, 1994.
7. Chambers SA. *Surf. Sci. Rep.* 2000; **39**: 105.
8. Goodman DW. *J. Vac. Sci. Technol., A* 1996; **14**: 1526.
9. Freund HJ. *Phys. Status Solidi B* 1995; **192**: 407.
10. Lopez-Carreno LD, Benitez G, Viscido L, Heras JM, Yubero F, Espinos JP, Gonzalez-Elipe AR. *Surf. Interface Anal.* 1998; **26**: 235.
11. Kottler V, Gillies MF, Kuiper AET. *J. Appl. Phys.* 2001; **89**: 3301.
12. Mozetic M, Zalar A, Cvelbar U, Babic D. *Surf. Interface Anal.* 2004; **36**: 986.
13. Maa JS, Meyerhofer D, O'Neill JJ Jr, White L, Zanzucchi PJ. *J. Vac. Sci. Technol., B* 1989; **7**: 145.
14. Romanyuk A, Oelhafen P, Melnik V. *Nucl. Instrum. Methods Phys. Res., Sect. B* 2005; **232**: 358.
15. Romanyuk A, Oelhafen P, Steiner R, Nellen PM, Reiner JC, Melnik V. *Surf. Sci.* 2005; **595**: 35.
16. Steigerwald JM, Murarka SP, Gutmann RJ. *Chemical Mechanical Planarization of Microelectronic Materials*. Wiley: New York, 1997.
17. Werheim GK, Dicenso SB. *J. Electron Spectrosc. Relat. Phenom.* 1985; **37**: 57.
18. Doniach S, Sunjic M. *J. Phys. C* 1970; **3**: 285.
19. Shirley DA. *Phys. Rev., B* 1972; **5**: 4709.
20. Lide DR. *Handbook of Chemistry and Physics* (72nd edn). CRC Press: Boston, MA, 1991.
21. Briggs D, Seah MP. *Practical Surface Analysis by Auger and X-Ray Photoelectron Spectroscopy*. Wiley: Chichester, 1983.
22. Lin TS, Partin WJ, Damminga GM, Parrill TM, Lee WJ, Chung YW. *Surf. Sci.* 1987; **183**: 113.
23. Gries WH. *Surf. Interface Anal.* 1996; **24**: 38.
24. Shigesato Y, Hayashi Y, Masui A, Haranou T. *Jpn. J. Appl. Phys.* 1991; **30**: 814.

Copyright © 2006 John Wiley & Sons, Ltd.

DOI: 10.1002/sia